Research Article/Araştırma Makalesi

GAZİ
JOURNAL OF ENGINEERING SCIENCES

Decision Support System for Blood Vessel and Optic Disc Segmentation

Cihan Akyel[*a], Nursal Arıcı[b]

Submitted: 12.09.2022 Revised: 03.12.2022 Accepted: 03.12.2022 doi:10.30855/gmbd.0705048

Keywords: LinkNet, Decision Support Systems, Deep Learning, ResNetC, Diabetes, Diabetic Retinopty

[a,*] Gazi University, Information Systems, Management Information Systems
06640 - Ankara, Türkiye
Orcid: 0000-0003-1792-8254
e mail: cihan.akyel1@gazi.edu.tr

[b] Gazi University, Applied Sciences Faculty, Management Information Systems
06560 - Ankara, Türkiye
Orcid: 0000-0002-4505-1341

[*]Corresponding author: cihan.akyel1@gazi.edu.tr

ABSTRACT

Diabetes mellitus has been on the rise recently. Diabetes can adversely affect different organs in the human body, along with blood flow. Diabetic retinopia is a type of diabetes that causes vision loss as a result of sugar destroying the vessels in the retina of the eye. Diabetic retinopia is one of the most important causes of blindness. Optic disc segmentation can help specialists in identifying these diseases. However, there are some obstacles, such as different brightness states on the images. Vessel noise can reduce segmentation success. This is because blood vessels can cut the edges of the optic disc. The aim in this study is to remove blood vessels from the images and then successfully segment the optic disc. Within the scope of the study, a new approach named LinkNetRCB7 based on LinkNet was developed. Successful results were obtained in the trainings made with LinkNetRCB7 data sets. The blood vessels and optic disc segmentation accuracy was 98.50% in the STARE dataset and 98.85% in the DRISHTI GS. A decision support system including these stages has been proposed within the scope of the study. There is no decision support system that includes deep learning and image processing algorithms for diabetic retinopia in the current literature.

Kan Damarı ve Optik Disk Bölütlemesi için Karar Destek Sistemi

ÖZ

Son zamanlarda şeker hastalığı hızla artmaktadır. Şeker hastalığı insan vücudunda farklı organları kan akışıyla birlikte olumsuz etkileyebilmektedr. Diyabetik retinopi, şekerin gözün retina tabakasındaki damaları tahrip etmesi sonucu görme kaybına neden olan bir diyabet türüdür. Diyabetik retinopi, körlüğün en önemli sebeplerindendir. Optik disk bölütlemesi bu hastalıkların belirlenmesinde uzmanlara yardımcı olabilmektedir. Ancak burada görüntüler üzerindeki farklı parlaklık durumları gibi bazı engeller ortaya çıkmaktadır. Damar gürültüsü bölütleme başarısını düşürebilmektedir. Bunun nedeni, kan damarlarının optik diskin kenarlarını kesebilmesidir. Bu çalışmada amaç, kan damarlarını görüntülerden çıkarmak ve ardından optik diski başarılı bir şekilde bölütlemektir. Çalışma kapsamında LinkNet'e dayalı LinkNetRCB7 adlı yeni bir yaklaşım geliştirildi. LinkNetRCB7 veri setleri ile yapılan eğitimlerde başarılı sonuçlar elde etmiştir. Kan damarları ve optik disk bölütleme doğruluğu, STARE veri setinde %98.50 ve DRISHTI GS'de %98.85 olarak hesaplandı. Bu aşamaları içeren bir karar destek sistemi çalışma kapsamında önerilmiştir. Mevcut literatürde diyabetik retinopi için derin öğrenme ve görüntü işleme algoritmalarını içeren bir karar destek sistemi görülmemektedir.

Anahtar Kelimeler: LinkNet, Karar Destek Sistemleri, Derin Öğrenme, ResNetC, Diyabet, Diyabetik Retinopati

To cite this article: C. Akyel and N. Arıcı, “Kan Damarı ve Optik Disk Bölütlemesi için Karar Destek Sistemi,” *Gazi Journal of Engineering Sciences*, vol. 9, no. 1, pp. 12-26, 2023. doi:10.30855/gmbd.0705048

1. Introduction

Diabetes is increasing rapidly throughout the world. There are about 650 million people affected by diabetes. Diabetic retinopathy is one of the types of diabetes. Diabetic retinotopia is an eye disease that can lead to blindness. Diabetes damages the blood vessels in the eye. This can lead to blood leakage. This leads to vision loss, blurred vision, or swelling [1]. By 2040, 600 million people will have diabetes and 200 million will have diabetic retinopathy [2]. DR is a leading cause of blindness in the United States. In 2020, there will be about 12000-24000 new cases annually. Diabetes is responsible for 40% of the total healthcare expenditure in the US [3]. Diabetic retinopathy can be prevented by early diagnosis. Experts can examine fundus images of the eyes to diagnose DR. However, there are many challenges, such as professionals' skills, contrast differences, image noise, and financial limitations [4]. The discovery of DR often occurs after severe damage has already occurred. In fact, visual examination is inferior in detecting vascular changes [5]. For these reasons, we need practical methods to detect diabetic retinopathy [6].

Experts can diagnose diabetic retinopathy using images segmented into the optic disc (OD). Computer-assisted methods such as image processing and deep learning can be used to perform ODS with high accuracy. However, blood interferes with the correct segmentation of OD. This is because OD may be subdivided by blood vessels. Thus, the vessels cover the optic nerve area [7]. Therefore, removal of this noise in fundus images is critical for ODS. Therefore, ODS and BVS are usually used in studies. The main challenge for the healthcare industry is to provide high- quality services at an affordable cost. Decision support systems (DSS) help the expert to make the right decision. DSS shorten the diagnosis time and increase the accuracy [8].

LinkNet is effective segmentation model. And it has some more succesful types such as LinkNetB7. There is no study that includes a decision support system with LinkNet on diabetic retinopaty in the literature. This paper presents in summary:

1. We presented a new model called LinkNetRCB7.
2. We used a way including deep learning and image processing algorithms.
3. A decision support system was developed in this study. Figure 1 illustrates proposed approach.

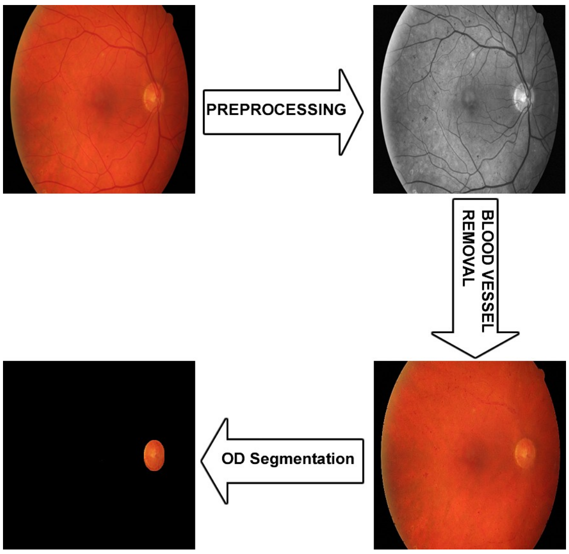

Figure 1. Overview of proposed approach

1.1. Related Works

In the literature, some studies used only image processing for segmentation. Maison et al. used a Gaussian filter based method for BVS. They used only image processing operations such as Clahe, morphological operations, and histogram equalization. They achieved 95.72% accuracy for the dataset DRIVE [9]. Image processing can be used for both mask correction and image segmentation. Shao et al. used kvsd-based kmeans as their method. Then they used pre- and post-processing for mask correction. In this way, small disturbances can be removed from the masks. In this study, an accuracy of 95.83% was calculated for BVS [10]. Millan and Marruga present a review of optic disk segmentation. They used the active contour technique (image processing). They achieved an accuracy of 85.67% [7]. Some studies do not use image processing for segmentation of blood vessels. Wang presents BTS-DSN that is based FCN. They achieved 0.8249% F1 in a rigid dataset. They used only the green channel to highlight non-specific vessels [11].

Image processing and deep learning are usually used together for better segmentation. Jiang et al. presented an MFI network based on the UNet. This study shows that the green channel has the highest accuracy. They used gamma correction and Clahe for preprocessing. Using the dataset STARE, an accuracy of 97.60% was achieved in BVS [12]. Yang et al. proposed LC-KSVD for BVS. They used preprocessing such as Clahe and bottom hat transformation. With Clahe, the blood vessels become more visible. Thus, algorithms can detect more easily. HRF, drive, and stare datasets were used. With the HRF dataset, they achieved 95.17% accuracy [13]. Another example of the combined use of image processing and Deep Learning is the RV-Net model proposed by Boudegga et al. In this study, an accuracy of 98.19% was achieved using the Drive dataset [14].
Correct removal of vascular noise from the image with predicted vascular masks is important to reduce losses. Inpaint functions are used for this purpose. Zhou et al. emphasize that vessels in retinal images affect segmentation accuracy. In this study, an inpainting algorithm with estimated blood vessel masks was used to obtain clean images. Then, optical segmentation was performed. Image processing and deep learning were used together. The cube coefficients (DI) were 95.5% for the DRISHTI-GS dataset for ODS [15]. In the study by Almazroa et al. an approach for segmentation of blood vessels was proposed. They used image processing algorithms such as top-hat filter and roi-based thresholding. Inpaint was used to fill voids corresponding to the masks. Segmentation of the optic disk was then performed. Using the Magrabi dataset, a cube accuracy of 90.1% was achieved [16].

In Deep Learning algorithms, overfitting is a problem that reduces the accuracy of training. Overfitting can be avoided by dividing the images into patches. In the study by Ma et al. this method was used. They proposed a WA mesh with residual blocks for BVS. They achieved an accuracy of 95.66% and an F1 score of 82.22% for the drive dataset [17]. Another study using patches was proposed by Browatzki et al. called Vlight. This model is based on Unet and Resnet. They achieved 96.71% on Chase [18].

The literature states that UNet is often preferred for BVS and ODS due to its high accuracy. Sanchez Brea et al. used UNET. They used the drive, stare, chase, RC-SLO, and IOSTAR datasets. They achieved 96% accuracy for IOSTAR and 97% for RC-SLO. Different numbers were used: 1, 10, 20 [19]. Lin et al. presented a study-based UNET. They achieved an accuracy of 96.08% for the hut. They mention a OD and fovea segmentation [20].

There are many studies based on UNet that improve the accuracy of education. Granley et al. have presented the HBA-UNet model. This model includes four resnet layers. A cube coefficient of 94.7% was obtained in the ADAM dataset and 94.7% in the REFUGE dataset. They calculated the effect of ResNet by 2% using UNet [6]. Laibacher et al. proposed a study. They developed M2U-Net: naming-based Unet. They used it to drive and chase datasets. In this study, they used Deep Learning to segment blood vessels. They achieved 80.91% dice accuracy on DRIVE and 80.06% on CHASE [21]. Lei et al. present Light Unet. In this work, a cube coefficient of 99.740 was obtained on the hut. ResNet-101 was used as the baseline network. In this study, the pooling layers were reduced to prevent the loss of important information [22]. Liu et al. proposed DDSC. DDSC is a model based on UNet. Cross entropy was used as the loss function. They achieved 97.80% on the DRISHTI-GS and 96.01% on the Refuge dataset [23].

The use of encoders improves the accuracy of image segmentation. This method is called transfer learning. Efficient types are effective models as encoders. Kamble et al. used Unet++ with efficientNetB4. In this study, the datasets REFUGE, DRISTHI-GS. and IDRiD were used. No dataset contains fovea and optic disk masks together. For this reason, the optic disk and fovea masks were merged. They achieved 95.73% accuracy in segmenting the optic disk with the Refuge dataset [24]. Lin et al. chose Resnet as the encoder. The main model was UNet for optic disk segmentation. They used image normalization and Clahe histogram equalization in the preprocessing step. These algorithms increase the contrast. This makes it easier to see the blood vessels in the image. They achieved 89.1% accuracy for the optic disk [25]. We can improve the contrast difference and segmentation accuracy by data normalization, gamma correction, and median filter. Jia et al. presented a model based on a dense U-mesh. They achieved 96.98% accuracy on a data set of DRIVE. They used images in the green channel. Then they used data normalization, gamma correction and median filter [26].

DSS can help clinicians by trying to guess the best probability among options. Recently, deep learning algorithms have been used for cancer detection in the model component of DSS [27]. Sivanesh et al. proposed a study titled DSS with data mining. They used the algorithm CART to classify various diseases such as heart and diabetes with datasets containing numerical values such as age, pain type, and serum cholesterol in mg/ [8]. In another study observers and observers in mammography reviews many studies, inter-variability is a critical problem and reduces this variability. They used Bayes for classification in DSS [28].

2. Materials and Methods

Study has two stages, blood vessel removal, and optic disc segmentation. In the blood vessel segmentation stage, we trained model with datasets. With the model trained at this stage, the data set used in the segmentation stage is cleaned of noise.

2.1. Datasets

The study consists of two phases: Segmentation of blood vessels and optic disc. We used CHASE (28 samples), DRIVE (20 samples), HRF (45 samples), and STARE (20 samples) datasets in the blood vessel removal phase. We merged these datasets into one dataset called Blood Vessel Dataset (BVD). The BVD contains 113 images and masks. For optic disc segmentation, we used ARIA (120 samples), DRISTHI-GS1 (101 samples), MESSIDOR (1200 samples), STARE (80 samples) and IDRiD (20 samples). We merged these datasets into a new dataset called Optic Disc Segmentation Dataset. The Optic Disc Segmentation Dataset (ODSD) contains 1420 images and masks. Table 1 demonstrates dataset distribution.

Table 1. Description of Datasets

Dataset	**Training (70%)**	**Validation (20%)**	**Test (10%)**
BVD	80	22	11
ODSD	1000	280	140

2.2. Image preprocess

We used data augmentation to prevent overfitting. This is another way to increase accuracy. Horizontal, vertical flips and shifts were applied. According to the literature, the studies generally use a maximum input size of 512x512, but the images in the datasets are larger. So there is pixel loss. For this reason, datasets were divided into 16 slices. And we used an input size of 256x256. So we have achieved an input size of 1024x1024.

2.2.1. Used filters and parameters

•Loss function: MSE (Mean Squared Error) + Dice Loss were used together. MSE measures the average of the squares of the errors [29]. Dice Loss decreases excessive segmentation errors, and the MSE reduces general image elaborations [30].

$$\text{LossFunction} = \text{MSEloss} + \text{DICEloss} \tag{1}$$

•Optimizer: We used The ADAMW optimizer ADAMW has better and faster results than ADAM [31]. We used weightDecay=0.05. With WeightDecay optimization algorithm decays the weight at each step of training.

2.2.2. Color channels

We used the median filter. It makes the images smoother. Then we divided all the images into RGB channels. As shown in Figure 2, the blood vessels are most visible in the green channel.

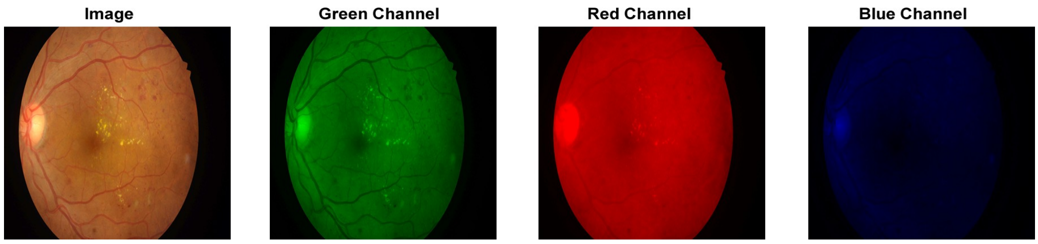

Figure 2. Images with Different Color Channels

2.2.3. Contrast enhancement

(4)

We convert images with the green channel to grayscale. The contrast is sharper in the green channel, after which normalization and Clahe (adaptive histogram equalization) were performed. Clahe was used in preprocessing to improve the contrast. Then Gaussian blur was used. It facilitates the detection of edges. With gamma correction, the image quality was increased (set to 1.2). Figure 3 shows the process.

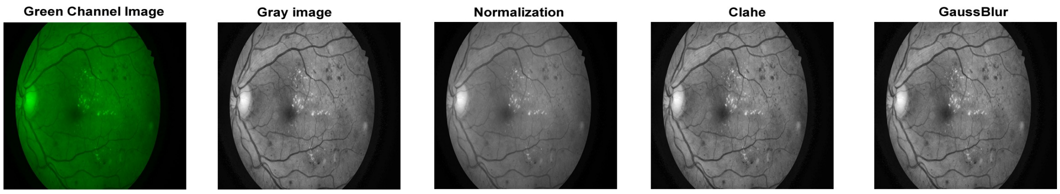

Figure 3. Contrast Enhancement Process

2.3. LinkNet

LinkNet uses batch normalization between convolutional layers followed by ReLU nonlinearity. This model uses an encoder-decoder structure. /2 means a stride of 2. LinkNet has eight blocks, four encoders, and four decoders [32]. The architecture of LinkNet is shown in Figure 7. The original LinkNet uses ResNet18 as the encoder. Compared to SegNet, ENet, Dilation10, VGG16, and ResNet101, LinkNet has the highest IoU. LinkNet is used for image segmentation [33]. LinkNet has high accuracy and a short epoch time. LinkNet has 11.5M parameters. There are studies according to which LinkNet has higher accuracy than UNet. According to Natarajan et al., LinkNet results better than UNet in segmentation [34].

2.4. EfficientnetB7 and ResNetC

The mobile inverted bottleneck is the main part of EffcientNet models [35]. Types of EfficientNet types have different numbers of this. EfficientNetB7 is the most successful model in EfficientNet types [36]. EfficientNetB7 can be seen in Figure 4. EfficientNet is generally used as an encoder in different types of segmentation. Chetoui et al. used EfficientNet in DR. They achieved successful results [37]. ResNetC includes 4 ResNet blocks. ResNetC network can be seen in Figure 5. ResNetC has almost 2 % higher dice accuracy than the basic ResNet architecture in the PH2 dataset [38].

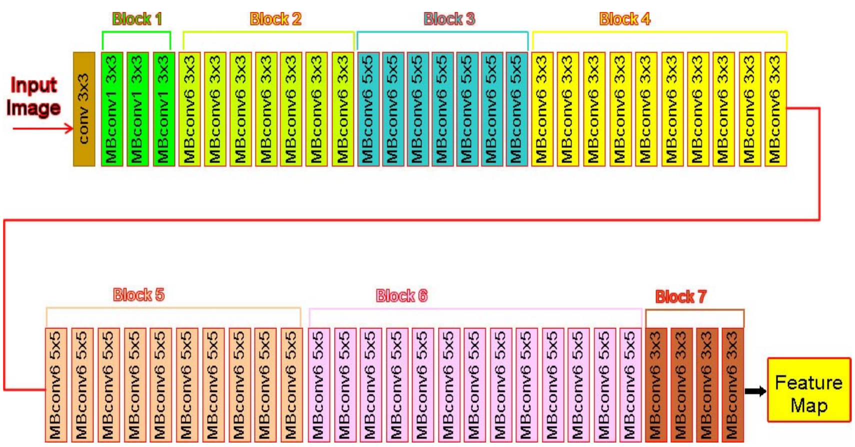

Figure 4. EfficientNetB7 Architecture

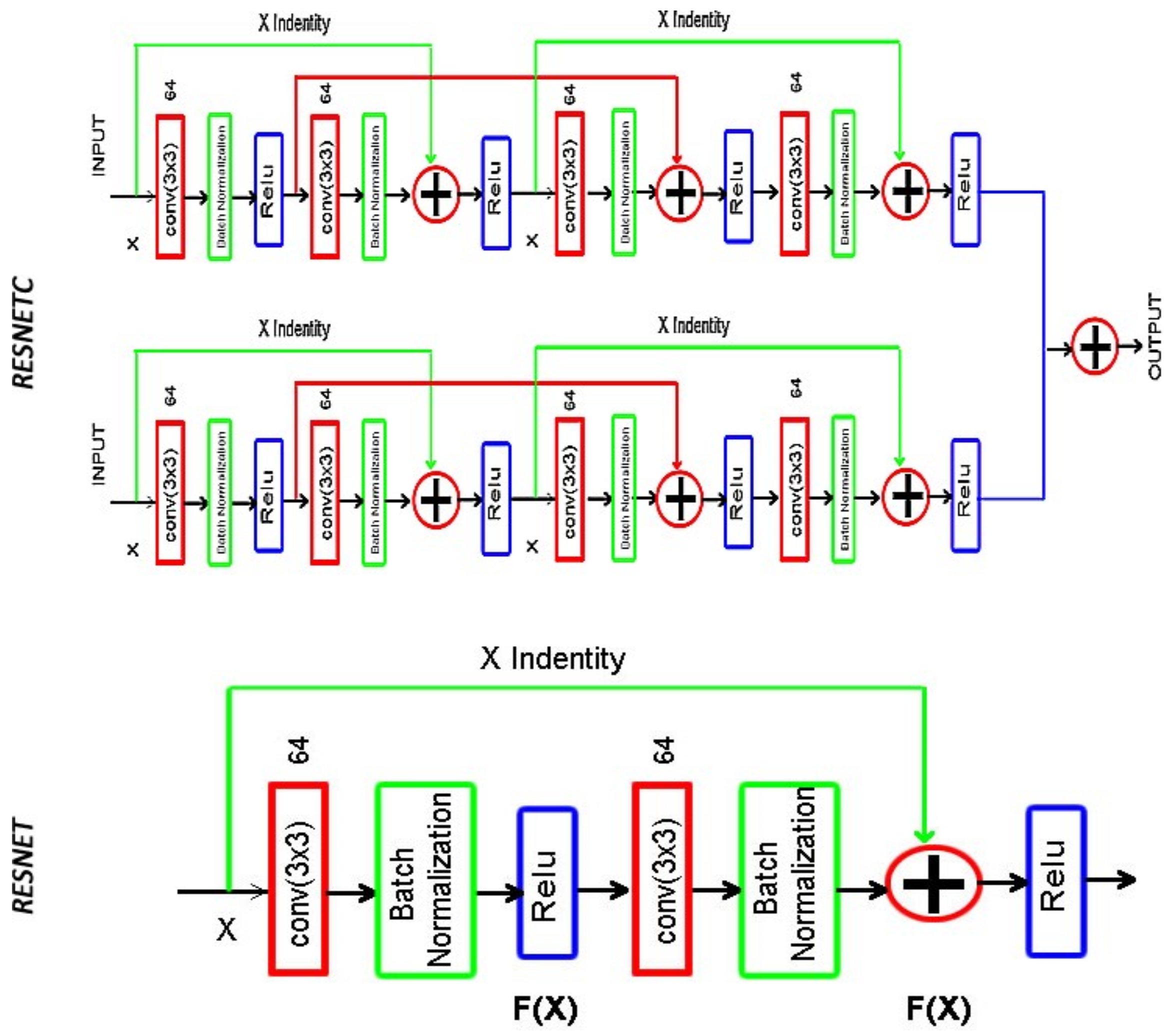

Figure 5. ResNet and ResNetC Architecture

2.5. Proposed model: LinkNet-RCB7

This model is based on LinkNetB7 [39]. We choose ADAMW. If there are potentially two classes, sigmoid is a suiTable output function [40]. Table 2 shows hyperparameters.

Table 2. Hyperparameters applied in models

Parameter	Blood Vessel Removal	Optic Disc Segmentation
Batch Size	16	16
Input Size	256	256
weightDecay	0.025	0.025
Learning Rate	0.001	0.001
Number of Epochs	500	500
Optimizer	ADAMW	ADAMW
Loss Function	MSE + Dice Loss	MSE + Dice Loss

EfficientNetB7 was chosen as the encoder. This is the best type among others (B0-B7) [41]. In this paper, a new model was presented named LinkNetRCB7. ResNetC blocks were used in the last layer and middle block. Thanks to this, more features can be obtained. Middle block contains 3 ResNetC blocks. With this block, accuracy increased by about 1%. In figure 6, proposed model can be seen. We used seven blocks that belong to EfficientnetB7.

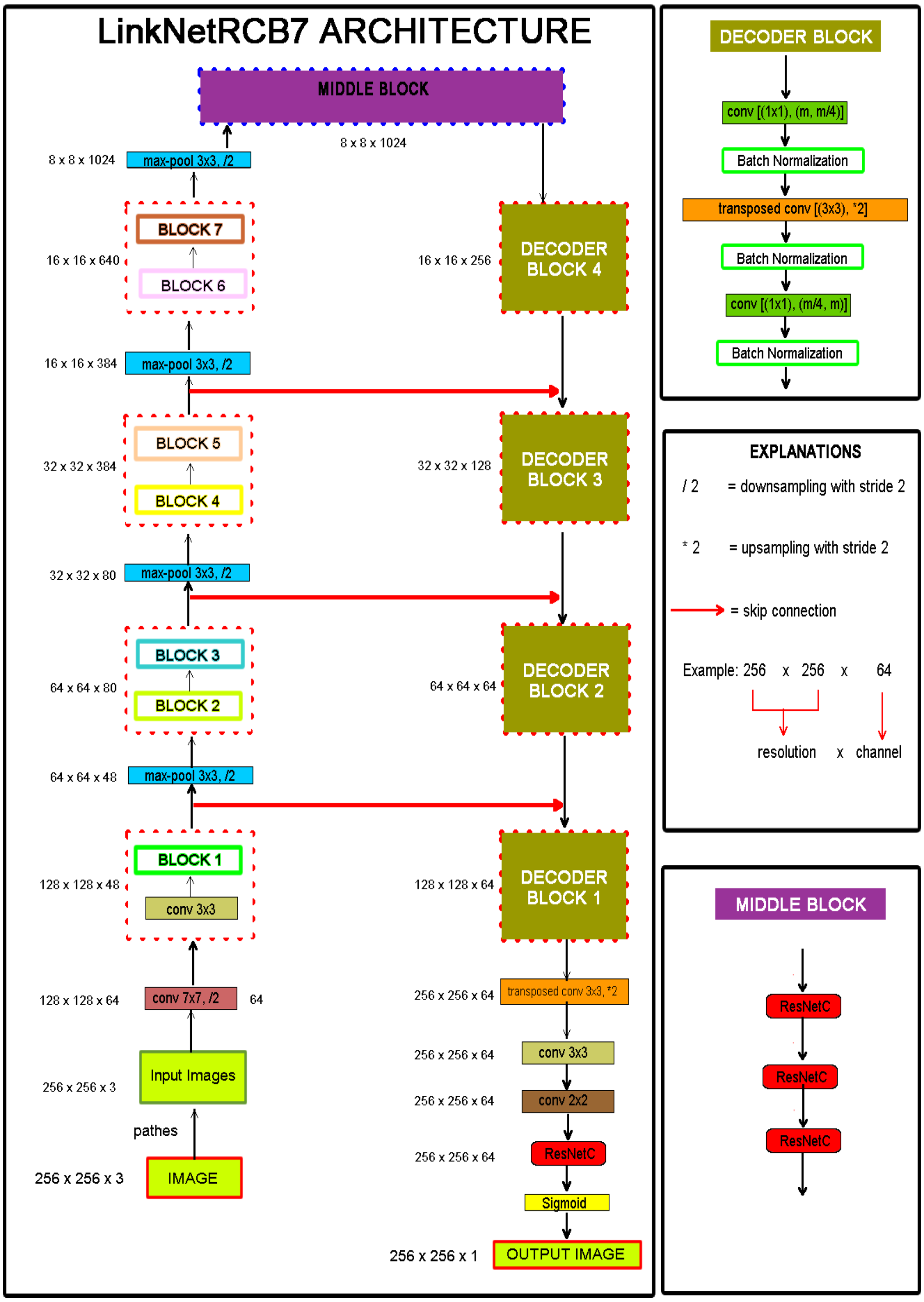

Figure 6. Proposed Model Architecture

2.6. Blood vessels removal

LinkNetRCB7 model was run with the blood vessel datasets. In the second stage, we used image processing. This allowed us to eliminate blood vessels by almost 99%. Figure 7 shows the process. Steps for the removal of blood vessels:

- The model was run for 500 epochs.
- We used morphological operations (opening, closing).
- Then we used the connectedComponentsWithStats function to remove small and unconnected objects.
- The test dataset was cleaned from noise using the model.

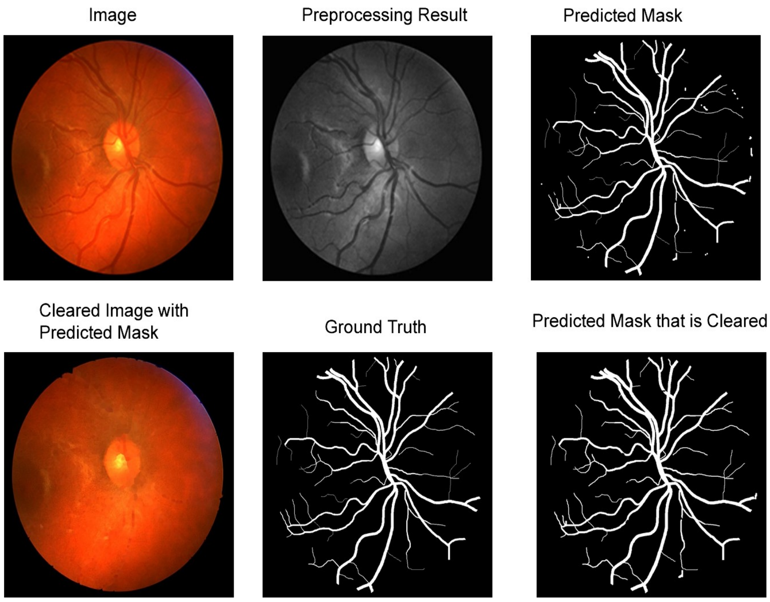

Figure 7. Blood Vessel Segmentation Stage Results

2.7. Optic disc segmentation

The dataset was cleared of noise in this step using a model trained in the blood vessel removal phase.

- The model was run for 500 epochs with the cleaned dataset.
- We used morphological operations (OPENING, CLOSING) to remove residual noise on the masks.
- Post-processing: the connectedComponentsWithStats function was used to remove small and unconnected objects.
- The test dataset was segmented with the trained model.

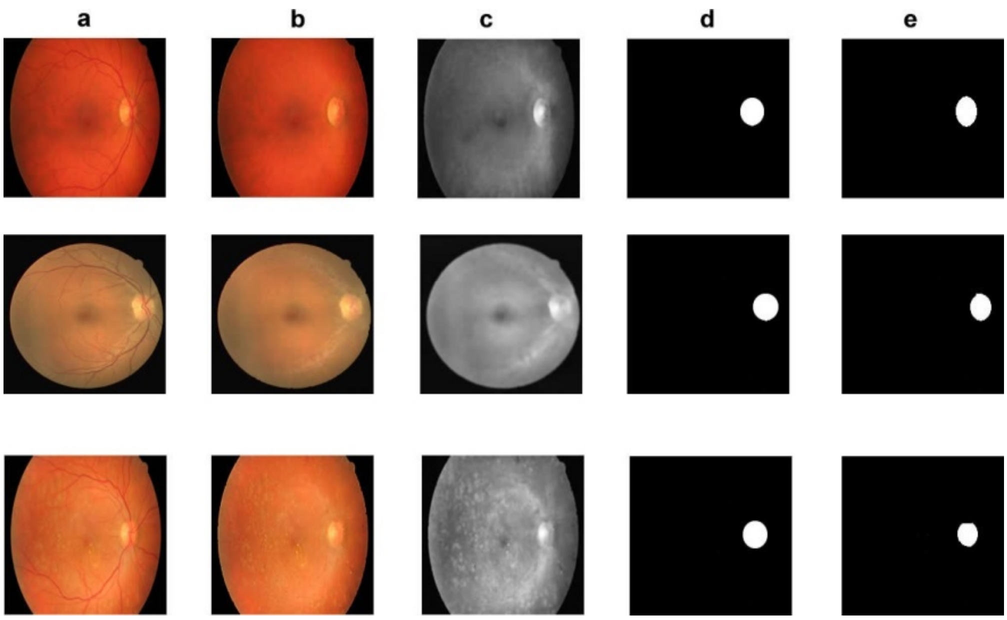

Figure 8. Optic Disc Segmentation Stage Results

3. Decision Support System

DSS helps decision-makers organize information and model outcomes. It is a computerized system that supports. A DSS consists of 3 components: GUI, data management, and model [42]. Disease to physician's decision support these systems based on classification algorithms that help diagnose systems. Clinical decision-making, such as diagnosis support systems based on patient data, are interactive software systems that help physicians [43]. In a study, DSS was designed to assist decision-makers [44]. In this research, the goal is to assist experts in making decisions. We have developed a DSS for blood vessel removal and optic disk segmentation in fundus images. This DSS can help experts in decision-making. It can also reduce diagnostic time and cost. The goal is to only help in diagnosis and not to make decisions instead of experts. In proposed DSS, seven different datasets were used. These datasets form the database part. They contain different sizes and numbers of images. LinkNetRCB7 is a model that was developed in this work.

We used Tkinter to develop a user interface for proposed model. It has a simple design to make it easy to use. There are three buttons. The "Load" button allows users to select images in .jpeg, jpg, gif, and png formats. Then pressing the "Remove Noise" button will remove the noise in the fundus images. Then the user can select a cleaned image or an image with noise. Finally, pressing the Segmentation button segments the selected image. We give users the choice of selecting noisy or clean images. If the experts think the removal phase is bad, they can choose another option. In summary, a user can do the following

1. Select the noisy or clean image with the LOAD button.
2. Remove blood vessels from the images.
3. Segmentation of the optic nerve head.
4. User can find three images as the report in the program folder. These are the original image, the cleaned image, and the segmented image.

In Figure 9, the general structure of proposed DSS can be seen. Figure 10 shows that the removal of noise and the segmentation process.

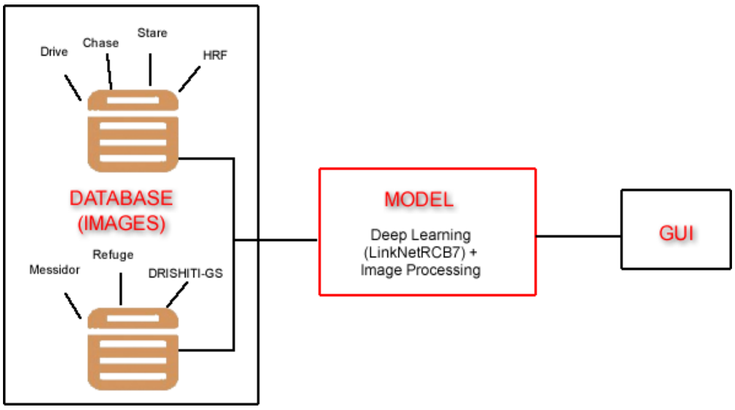

Figure 9. Structure of Proposed DSS

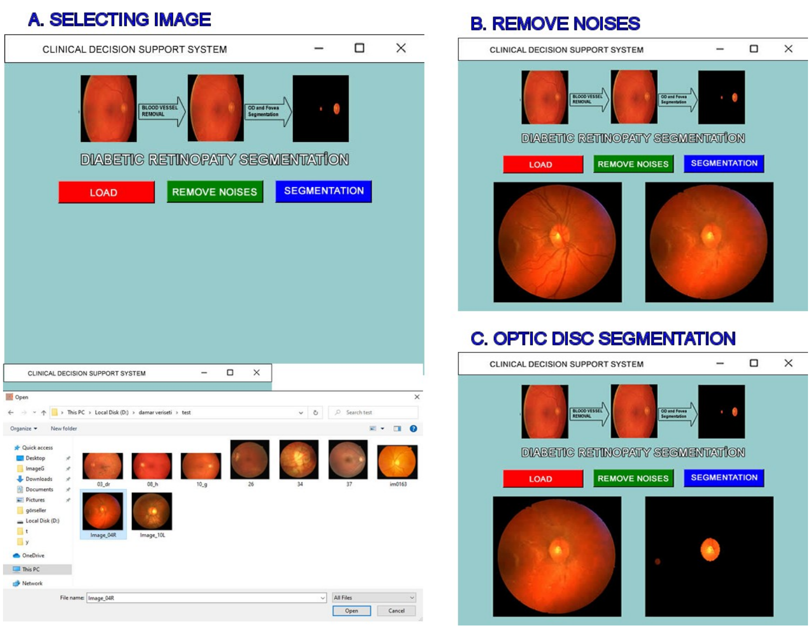

Figure 10. Gui of Proposed DSS

4. Results

4.1. Results of blood vessel segmentation

Different models were used in training stage. Table 3 demonstrates blood vessel segmentation results. Table 4 compares studies (DI= Dice coefficient, ACC: Accuracy, S.E.: Sensitivity, S.P.: Specificity). These studies uses different datasets. Because of this, the proposed model has run with the different dataset to correct comparisons.

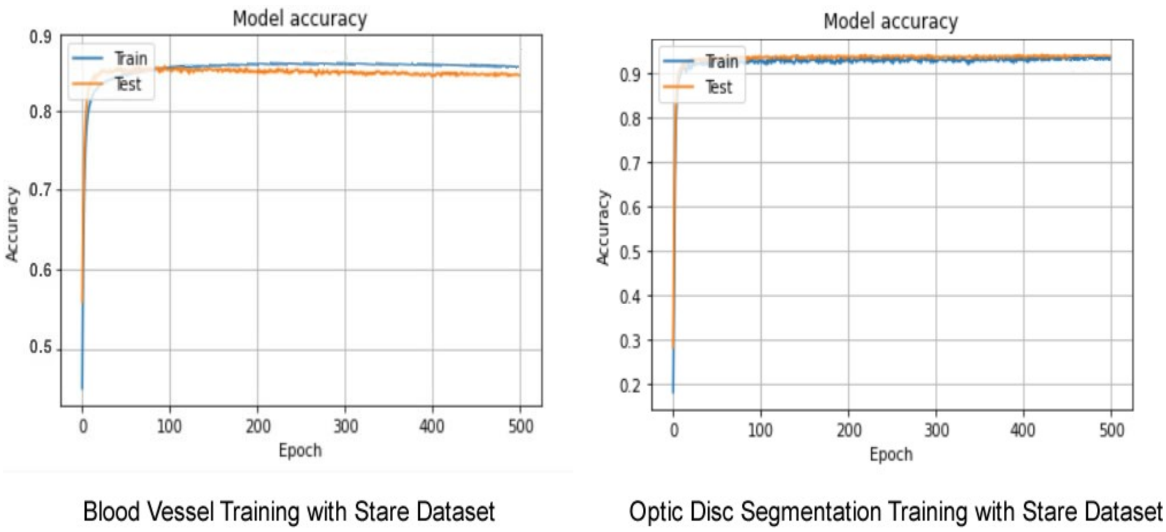

Figure 11. Graphics of Training.

Table 3. Blood Vessel Segmentation

Model	ACC	mIoU	DI	SE	S.P.	F1	Dataset
UNet	93.80	80.50	79.70	80.55	96.30	81.00	Stare
UNet++	96.20	82.30	80.70	82.15	97.20	82.70	Stare
C-Net	96.70	83.10	82.80	83.20	98.10	83.70	Stare
LinkNetB7	97.20	84.60	83.10	86.30	98.30	84.10	Stare
Proposed Model	97.95	84.20	85.40	87.20	98.30	86.25	Drive
Proposed Model	97.60	83.65	84.50	86.30	97.40	86.20	Chase
Proposed Model	**98.50**	**85.85**	**85.75**	**88.10**	**99.40**	**86.50**	**Stare**
Proposed Model	97.50	83.30	84.10	86.80	97.80	84.30	HRF
Proposed Model	96.30	82.20	85.00	85.30	96.70	83.50	BVD

Table 4. Comparison of Models in Blood Vessel Segmentation

	DRIVE			CHASE			STARE			HRF		
Refe-rence	**Acc**	**F1**	**DI**	**Acc**	**F1**	**DI**	**Acc**	**F1**	**DI**	**Acc**	**F1**	**DI**
[12]	97.05	83.18	–	**97.62**	81.50	–	97.66	84.83	–	–	–	–
[17]	95.66	82,22	–	–	–	–	96.45	82.23	–	–	–	–
[21]	96.30	–	80.91	97.03	–	80.06	–	–	–	–	–	–
[13]	94.21	76.73	–	–	–	–	94.77	72.60	–	95.17	74.49	–
[9]	95.72	–	–	–	–	–	–	–	–	–	–	–
[14]	**98.19**	–	–	–	–	–	98.16	–	–	–	–	–
[19]	92.00	–	71.00	95.00	–	74.00	95.00	–	69.00	93.00	–	60.00
[18]	95.65	82.99	–	96.71	81.94	–	–	–	–	–	–	–
[10]	95.83	75.45	–	–	–	–	95.31	69.04	–	95.49	70.93	–
[26]	96.98	–	–	–	–	–	–	–	–	–	–	–
[11]	95.61	82.49	–	96.27	79.83	–	96.74	84.21	–	–	–	–
Proposed	97.95	**86.25**	**85.40**	97.60	**86.20**	**84.50**	**98.50**	**86.50**	**85.75**	**97.50**	**84.30**	**84.10**

For blood vessel segmentation, we used different datasets in cross-training. Table 5 demonstrates obtained results. And figure 12 indicates predicted masks with other models.

Table 5. Cross-training test results in blood vessel segmentation

	TRAIN DATASETS							
	DRIVE		**CHASE**		**STARE**		**HRF**	
Test Dataset	Acc	DI	Acc	DI	Acc	DI	Acc	DI
DRIVE	–	–	94.15	81.70	96.90	84.15	96.30	83.75
CHASE	96.10	83.40	–	–	96.00	84.00	95.75	82.80
STARE	97.00	84.20	95.50	83.10	–	–	96.40	83.95
HRF	96.00	83.20	93.80	81.65	95.80	83.85	–	–

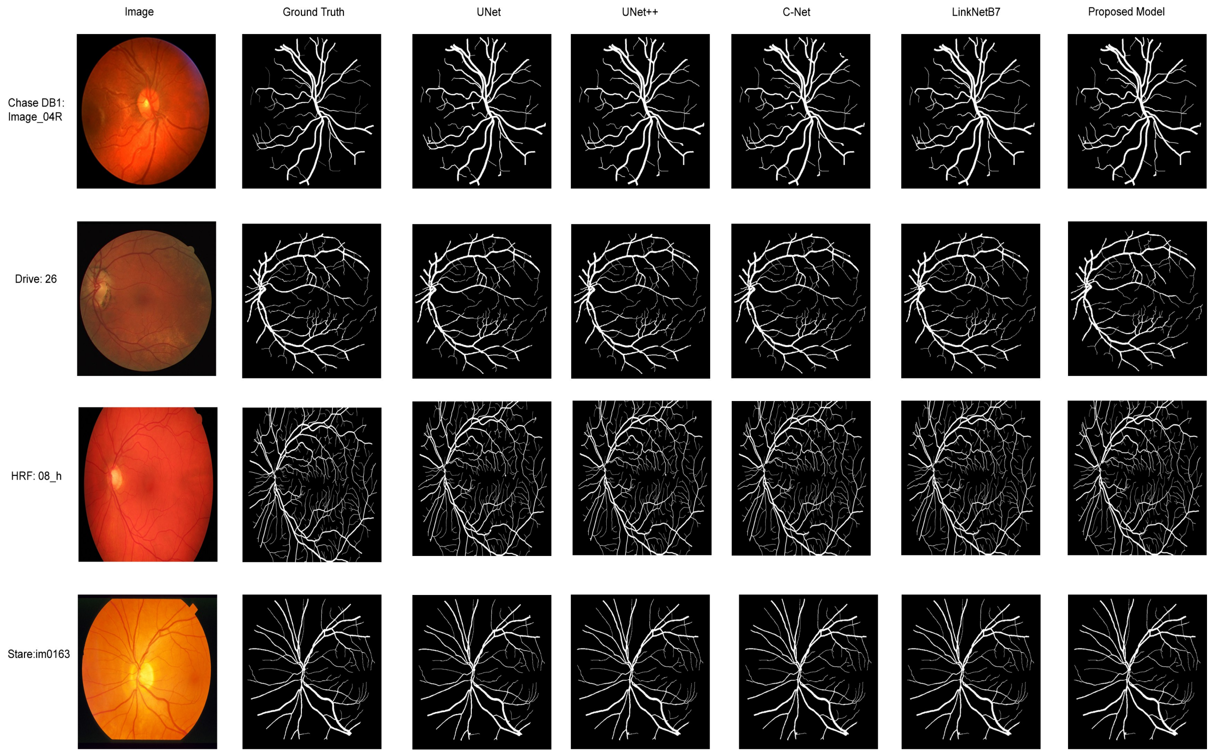

Figure 12. Mask Predictions of Blood Vessel Segmentation with Different Models

4.2. Results of optic disc segmentation

We used five models in the training stages. Table 6 shows the results of these models with different datasets. Table 7 demonstrates the comparison of studies. Table 8 shows the results of the cross-training tests.

Table 6. Optic Disc Segmentation

Model	**ACC**	**mIoU**	**DI**	**SE**	**S.P.**	**F1**	**Dataset**
UNet	93.85	90.20	92.80	92.70	95.10	93.20	DRISHTI-GS
UNet++	96.15	92.10	94.60	94.40	96.50	95.05	DRISHTI-GS
C-Net	96.25	92.20	95.30	94.90	97.10	95.50	DRISHTI-GS
LinkNetB7	98.10	93.80	96.60	96.40	98.50	97.40	DRISHTI-GS
Proposed	98.65	93.40	98.00	97.10	98.75	98.00	ARIA
Proposed	95.95	91.20	94.40	95.60	95.90	96.00	MESSIDOR
Proposed	98.25	93.05	98.10	97.30	98.80	97.75	REFUGE
Proposed	**98.85**	**93.50**	**98.30**	**97.50**	**99.10**	**98.00**	**DRISHTI-GS**
Proposed	97.50	92.30	97.25	96.10	97.80	97.35	ODSD

Table 7. Comparison of Optic Disc Segmentation

	DRISHTI-GS			**REFUGE**			**MESSIDOR**		
Reference	**ACC**	**DI**	**mIoU**	**ACC**	**DI**	**mIoU**	**ACC**	**DI**	**mIoU**
[23]	–	97.80	–	–	96.01	–	–	- -	–
[24]	–	–	–	–	94.70	–	–	–	–
[6]	–	97.84	–	–	95.73	–	–	–	–
[15]	–	95.50	–	–	–	–	–	–	–
[16]	–	–	–	–	–	–	86.60	–	–
[22]	–	**99.74**	93.26	–	**98.22**	88.53	–	–	–
[20]	–	–	–	–	96.08	–	–	–	–
Proposed	**98.85**	98.30	**93.50**	**98.25**	97.75	**93.05**	**95.95**	**96.00**	**91.20**

Table 8. Cross-training test results in optic disk segmentation

	TRAIN DATASETS							
	DRISHTI-GS		REFUGE		MESSIDOR		ARIA	
Test Dataset	Acc	DI	Acc	DI	Acc	DI	Acc	DI
DRISHTI-GS	–	–	**98.10**	**97.25**	**95.60**	**94.20**	**98.40**	**98.00**
REFUGE	**98.70**	97.80	–	–	94.80	94.00	98.30	97.80
MESSIDOR	96.00	95.00	96.50	96.40	93.70	93.20	96.90	96.30
ARIA	98.50	**97.85**	97.10	96.90	94.20	93.80	–	–

Figure 13 demonstrates predicted masks with different models.

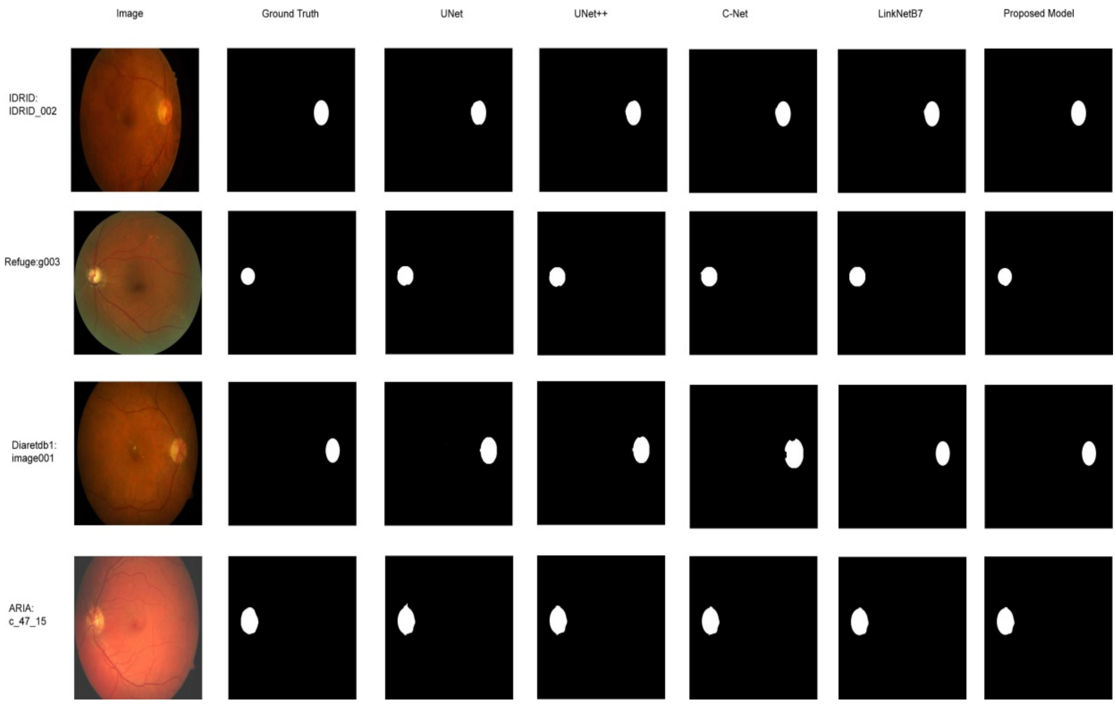

Figure 13. Mask Predictions of Optic Disc Segmentation with Different Models.

4.3. Ablation studies

We chose LinkNet as the base model. Then we add the EfficientNetB7 and ResNetC models to the base model and look at their effects on the base model. We used Accuracy, F1, MeanIoU, and Dice Accuracy and presented the test results in Tables 9 and 10.

Table 9. Ablation Study in Blood Vessel Removal Stage with BVD Dataset

Parameter	ACC	meanIoU	DI	F1
Baseline model	90.25	77.00	79.22	77.80
Baseline model + ResNet	91.05	78.35	80.20	78.75
Baseline model + ResNetC	92.20	79.15	81.10	79.45
Baseline model + EfficienNetB7	95.40	82.25	84.10	82.30
Baseline model + EfficienNetB7 + ResNet	95.60	81.75	84.60	83.00
Baseline model + EfficienNetB7 + ResNetC	**96.30**	**82.20**	**85.00**	**83.50**

Table 10. Ablation Study in Lesion Segmentation Stage with ODSD dataset

Parameter	ACC	meanIoU	DI	F1
Baseline model	94.00	89.30	93.90	93.00
Baseline model + ResNet	94.30	89.70	94.10	93.30
Baseline model + ResNetC	94.50	90.00	94.40	93.60
Baseline model + EfficienNetB7	96.50	91.20	96.00	95.70
Baseline model + EfficienNetB7 + ResNet	97.00	91.90	96.70	96.20
Baseline model + EfficienNetB7 + ResNetC	**97.50**	**92.30**	**97.25**	**97.35**

5. Conclusion

In this study LinkNetRCB7 was developed for image segmentation. This model has obtained successful results. In blood vessel segmentation, the proposed model is the most successful model except for two studies on only accuracy parameter. It is seen in the literature that vessel noise becomes more prominent in the green color channel. Therefore, the green color channel was preferred in the study and increased success was achieved.

In ODS, the proposed model has also good results. As a result, this study proposed a DSS with a new model called LinkNet-RC7. High accuracy values were obtained in BVS and ODS stages. There is no such study in the literature that includes DSS with ODS and BVS. These and similar studies may be promising for the early diagnosis of diabetic retinopia.

In future studies, pixel loss can be further reduced by increasing the number of slices. In addition, comparisons can be made by experimenting with different color spaces such as HSV for the images to be trained.

Conflict of Interest Statement

The authors declare that there is no conflict of interest.

References

[1] K. P. Mali, B. T. Jadhav and I. K. Mujawar. "Study of Diabetic retinopaty Detection Using Deep Learning Techniques," *International Research Journal of Humanities and Interdisciplinary Studies Journal*, Special Issue, pp. 208-216, March 2022. doi:03.2021-11278686

[2] Y. Guo and Y. Peng. "CARNet: Cascade attentive RefineNet for multi-lesion segmentation of diabetic retinopaty images," *Complex Intelligent Systems*, vol.8, pp. 1681–1701, January 2022. doi:10.1007/s40747-021-00630-4

[3] S. E. Mansour, D. J. Browning, K. Wong, H. W. Flynn and A. R. Bhavsar. "The Evolving Treatment of Diabetic retinopaty," *Clin Ophthalmol*, vol.14, pp. 653–678, March 2020. doi:10.2147/OPTH.S236637

[4] G. Zhang, B. Sun, Z. Chen, Y. Gao, Z. Zhang, W. Yang and K. Li. "Diabetic retinopaty Grading by Deep Graph Correlation Network on Retinal Images Without Manual Annotations," *Frontiers in Medicine*, vol.9, pp. 1-9, April 2022. doi:10.3389/fmed.2022.872214

[5] S. H. Sinclair and S. S. Schwartz. "Diabetic retinopaty–An Underdiagnosed and Undertreated Inflammatory, Neuro Vascular Complication of Diabetes," *Frontiers in Medicine*, vol.10, December 2019. doi:10.3389/fendo.2019.00843

[6] S. Tang, Z. Qi, J. Granley and M. Beyeler. "U-Net with Hierarchical Bottleneck Attention for Landmark Detection in Fundus Images of the Degenerated Retina*," in Proc. of International Workshop on Ophthalmic Medical Image Analysis," 27 September 2021*, Strasbourg, France, [Online]. Available: https://www.researchgate.net/publication/354724454_U-Net_with_Hierarchical_Bottleneck_Attention_for_Landmark_Detection_in_Fundus_Images_of_the_Degenerated_Retina. [Accessed: Dec, 5, 2022].

[7] A. G. Marrugo and M. S. Millan. "Optic disc segmentation in retinal images," *https://iopscience.iop.org/,* 2011, [Online]. Avaliable: https://iopscience.iop.org/article/10.1088/1742-6596/274/1/012039/pdf. [Accessed: Nov, 15, 2022]

[8] S. Kumar, G. Sathyadevi and S.Sivanesh. "Decision Support System for Medical Diagnosis Using Data Mining," *researchgate.net*,
May. 2011, [Online]. Avaliable: https://www.researchgate.net/publication/267934132_Decision_Support_System_for_Medical_Diagnosis_Using_Data_Mining. [Accessed Dec, 5, 2022]

[9] M. Maison, T Lestari and A. Luthfi. "Retinal Blood Vessel Segmentation using Gaussian Filter," *https://iopscience.iop.org/,* 2019, [Online]. Avaliable: https://iopscience.iop.org/article/10.1088/1742-6596/1376/1/012023 [Accessed: Dec, 5, 2022]

[10] Y. Yang, F. Shao, Z. Fu and R. Fu. "Blood vessel segmentation of fundus images via cross-modality dictionary learning," *Applied Optics*, vol. 57, no. 25, September 2018. doi:10.1364/AO.57.007287

[11] S. Guo, K. Wang, H. Kang, Y. Zhang, Y. Gao and T. Li, "BTS-DSN: Deeply Supervised Neural Network with Short Connections for Retinal Vessel Segmentation," *International Journal of Medical Informatics*, vol. 126, pp. 105-113, June 2019. doi:10.1016/j.ijmedinf.2019.03.015

[12] Y. Jiang, C. Wu, G. Wang, H. Yao, and W. Liu. "MFI-Net: A multi-resolution fusion input network for retinal vessel segmentation," *PLOS ONE*, vol. 16, no. 7, May 2021. doi:10.1007/s11760-019-01501-9

[13] Y. Yang, F. Shao, Z. Fu and R. Fu. "Discriminative dictionary learning for retinal vessel segmentation using fusion of multiple features," *Signal, Image and Video Processing*, vol.13, pp. 1529–1537, 2019.

[14] H. Boudegga, Y. Elloumi, M. Akil, M. H. Bedoui, R. Kachouri and A. B. Abdallah, "Fast and efficient retinal blood vessel segmentation method based on deep learning network," *Computerized Medical Imaging and Graphics*, vol. 90, June 2021. doi:10.1016/j.compmedimag.2021.101902

[15] W. Zhou, Y. Yi, Y. Gao and J. Dai. ”Optic Disc and Cup Segmentation in Retinal Images for Glaucoma Diagnosis by Locally Statistical Active Contour Model with Structure Prior,” *Hindawi Computational and Mathematical Methods in Medicine*, vol. 2019, 2019. doi:10.1155/2019/8973287

[16] A. Almazroa, W. Sun, S. Alodhayb, K. Raahemifar and V. Lakshminarayanan, ”Optic disc segmentation for glaucoma screening system using fundus images,” *Clinical Ophthalmology,* vol. 2017, pp. 2017-2029, November 2017. doi:10.2147/OPTH.S140061

[17] Y. Ma, X. Li, X. Duan, Y. Peng and Y. Zhang. ”Retinal Vessel Segmentation by Deep Residual Learning with Wide Activation,” *Hindawi Computational Intelligence and Neuroscience*, vol. 2020, 2020. doi:10.1155/2020/8822407

[18] B. Browatzki, J. Lies and C. Wallraven, ”Encoder-Decoder Networks for Retinal Vessel Segmentation Using Large Multi-scale Patches,” *dl.acm.org*, oct. 2020, [Online]. Avaliable: https://dl.acm.org/doi/abs/10.1007/978-3-030-63419-3_5. [Accessed: Sept, 10, 2022].

[19] L. S. Brea, D. A. De Jesus, S. Klein and T. V. Walsum, ”Deep learning-based retinal vessel segmentation with cross-modal evaluation,” *proceedings.mlr.press,* 2020, [Online]. Avaliable: http://proceedings.mlr.press/v121/sanchez-brea20a/sanchez-brea20a.pdf. [Accessed: Sept, 5, 2022].

[20] H. He, L. Lin, X. Tang and Z. Cai, ”JOINED: Prior Guided Multi-task Learning for Joint Optic Disc/Cup Segmentation and Fovea Detection,” *arxiv.org*, 1 March. 2022, [Online]. Avaliable: https://arxiv.org/abs/2203.00461 [Accessed: Sept, 5, 2022].

[21] T. Laibacher, T. Weyde and S. Jalali. ”M2U-Net: Effective and Efficient Retinal Vessel Segmentation for Real-World Applications,” *in Proc. Of IEEE/CVF Conference on Computer Vision and Pattern Recognition Workshops (CVPRW), 16-17 June 2019,* Long Beach, CA, USA [Online]. Avaliable: https://arxiv.org/abs/1811.07738. [Accessed: Sept, 5, 2022].

[22] W. Liu, H. Lei, H. Xie, B. Zhao, G. Yue and B. Lei, ”Multi-level Light U-Net and Atrous Spatial Pyramid Pooling for Optic Disc Segmentation on Fundus Image,” *in Proc. of Ophthalmic Medical Image Analysis 7th International Workshop, 8 oct 2020*, Lima, Peru [Online]. Avaliable: https://link.springer.com/chapter/10.1007/978-3-030-63419-3_11. [Accessed: Sept, 5, 2022].

[23] B. Liu, D. Pan and H. Song, ”Joint optic disc and cup segmentation based on densely connected depthwise separable convolution deep network,” *BMC Medical Imaging*, vol.21, no.14, January 2021. Doi: 10.1186/s12880-020-00528-6.

[24] R. Kamble, P. Samanta and N. Singhal, Optic Disc, ”Cup and Fovea Detection from Retinal Images Using UNet++ with EfficientNet Encoder,” *in Proc. of the International Workshop on Ophthalmic Medical Image Analysis, 8 October 2020*, Lima, Peru. [Online]. Avaliable: https://link.springer.com/chapter/10.1007/978-3-030-63419-3_10 [Accessed: Dec, 7, 2022].

[25] J. Lin, X. Liao, L. Yu and J. Pan, ”Res-UNet Based Optic Disk Segmentation in Retinal Image,” *Journal of Computers,* vol. 31 no. 3, pp. 183-194, March 2020. doi:10.3966/199115992020063103014

[26] Z. Li, M. Jia, X. Yang and M. Xu, ”Blood Vessel Segmentation of Retinal Image Based on Dense-U-Net Network,” *Micromachines,* vol. 12, no. 12, December 2021. doi:10.3390/mi12121478

[27] H. Ucuzal, ”Yapay Zekâya Dayalı Anlamsal Video İşleme Yöntemlerinin Tıpta Kullanılabilirliğinin Araştırılması,” Yüksek Lisans Tezi, Sağlık Bilimleri Enstitüsü, Biyoistatistik ve Tıp Bilişimi Anabilim Dalı, İnönü Üniversitesi, Malatya, Türkiye, 2020.

[28] S. Bozkurt, ”Gerçek Zamanlı Mamografi Yorumu Karar Destek Sistemi,” Doktora Tezi, Sağlık Bilimleri Enstitüsü, Biyoistatistik ve Tıbbi Bilişim Anabilim Dalı, Akdeniz Üniversitesi, Antalya, Türkiye, 2015.

[29] Y. Park, ”Concise Logarithmic Loss Function for Robust Training of Anomaly Detection Model,” *arxiv.com,* 15 Jan. 2022, [Online]. Avaliable: https://arxiv.org/abs/2201.05748. [Accessed: Dec, 7, 2022].

[30] N. Savioli, G. Montana and P. Lamata, ”V-FCNN: Volumetric Fully Convolution Neural Network For Automatic Atrial Segmentation,” *in Proc. of International Workshop on Statistical Atlases and Computational Models of the Heart, 14 Feb. 2019,* Granada, Spain. [Online]. Avaliable: https://arxiv.org/pdf/1808.01944.pdf. [Accessed: Dec, 7, 2022].

[31] I. Loshchilov and F. Hutter, ”DECOUPLED WEIGHT DECAY REGULARIZATION,” *in Proc. ICLR 2019 Conference homepage, 6-9 May. 2019,* New Orleans, Louisiana, United States. [Online]. Avaliable: https://arxiv.org/abs/1711.05101. [Accessed: Sept, 17, 2022].

[32] L. Zhou, C. Zhang and M. Wu. “D-LinkNet with Pretrained The encoder and Dilated Convolution for Resolution Satellite Imagery Road Extraction,” *in Proc. of the 2018 IEEE/CVF Conference on Computer Vision and Pattern Recognition Workshops (CVPRW), 18–22 June 2018,* Salt Lake City, UT, USA. [Online]. Avaliable: https://ieeexplore.ieee.org/document/8575492. [Accessed: Sept, 7, 2022].

[33] A. Chaurasia and E. Culurciello. “LinkNet: Exploiting The encoder Representations for Efficient Semantic Segmentation,” *in Proc. of the IEEE Visual Communications and Image Processing (VCIP), 10–13 December 2017*, St. Petersburg, FL, USA. [Online]. Avaliable: https://arxiv.org/abs/1707.03718. [Accessed: Sept,1 7, 2022].

[34] S. Kallam, M. S. Kumar, V. A. Natarajan and R. Patan. “Segmentation of Nuclei in Histopathology images using Fully Convolutional Deep Neural Architecture,”. *in Proc. of the 2020 International Conference on Computing and Information Technology (ICCIT-1441), 23 November 2020,* Tabuk, Saudi Arabia. [Online]. Avaliable: https://ieeexplore.ieee.org/document/9213817. [Accessed: Sept, 17, 2022].

[35] M. Sandler, A. G. Howard, M. Zhu, A. Zhmoginov and L. Chen. “Mobilenetv2: Inverted residuals and linear bottlenecks *in Proc. of* the 2018 IEEE/CVF Conference on Computer Vision and Pattern Recognition, 18–23 June 2018, Salt Lake City, UT, USA. [Online]. Avaliable: https://arxiv.org/abs/1801.04381. [Accessed: Dec, 7, 2022].

[36] T. Mingxing and V. L. Quoc. “EfficientNet: Rethinking Model Scaling for Convolutional Neural Networks*,” in Proc. of the 36th International Conference on Machine Learning, 9–15 June 2019,* Long Beach, CA, USA. [Online]. Avaliable: https://arxiv.org/abs/1905.11946. [Accessed: Dec, 7, 2022].

[37] M. Chetoui and M. A. Akhloufi. “Explainable Diabetic retinopaty using EfficientNET,” *in Proc. of the 42nd Annual International Conference of the IEEE Engineering in Medicine Biology Society (EMBC),* 20–24 July 2020, Montreal, QC, Canada. [Online]. Avaliable: https://pubmed.ncbi.nlm.nih.gov/33018388/ [Accessed: Sept, 15, 2022].

[38] C. Akyel ve N. Arıcı, ”Hair Removal and Lesion Segmentation with FCN8- ResNetC and Image Processing in Images of Skin Cancer,” *Journal of Information Technologies*, vol. 15, no. 2, pp. 231-238, 2022. doi:10.17671/gazibtd.1060330

[39] C. Akyel ve N. Arıcı, ”LinkNet-B7: Noise Removal and Lesion Segmentation in Images of Skin Cancer,” *Mathematics,* vol. 10, no. 5, pp. 736-751. doi:10.3390/math10050736

[40] L. Nieradzik, G. Scheuermann, B. Saur and C. Gillmann, “Effect of the output activation function on the probabilities and errors in medical image segmentation,” *arxiv.org,* 2 Sept. 2021, [Online]. Avaliable: https://arxiv.org/pdf/2109.00903.pdf [Accessed: Dec, 7, 2022].

[41] W. Xiong, X. Jia, D. Yang, M. Ai, L. Li and S. Wang. “DP-LinkNet: A convolutional network for historical document image binarization,”. *Internet Information Systems,* vol. 15, no. 5, pp. 1778–1797, May 2021. doi:10.3837/tiis.2021.05.011

[42] M. Dönerçark ve V. Tecim, ”Kurumsal Karar Destek Sistemlerinde Yapay Zeka Kullanımı: Tasarım ve Uygulama,” d*ergipark.org.tr,* 2020, [Online]. Avaliable: https://dergipark.org.tr/tr/pub/ybs/issue/58550/821708#article_cite [Accessed: Sept, 15, 2022].

[43] I. Çakmak, ”Makine Öğrenmesi Yöntemleriyle Tümör Kontrol Olasılığının Hesaplanması, Yüksek Lisans Tezi, Sağlık Bilimleri Enstitüsü, Biyoistatistik ve Tıbbi Bilişim Anabilim Dalı, Karadeniz Teknik Üniversitesi, Trabzon, Türkiye, 2017.

[44] M. E. Çorapçıoğlu, ”Tıpçıt: Tıbbi Karar Destek Sistemi Çekirdeği,” Yüksek Lisans Tezi, Bilgisayar Mühendisliği Anabilim Dalı, Başkent Üniversitesi, Ankara, Türkiye, 2006.